

# Balancing Biases and Preserving Privacy on Balanced Faces in the Wild

Joseph P Robinson, *Member, IEEE*, Can Qin, *Student Member, IEEE*, Yann Henon, Samson Timoner, *Member, IEEE*, and Yun Fu, *Fellow, IEEE*

**Abstract**—There are demographic biases in current models used for facial recognition (FR). Our Balanced Faces In the Wild (BFW) dataset serves as a proxy to measure bias across ethnicity and gender subgroups, allowing one to characterize FR performances per subgroup. We show results are non-optimal when a single score threshold determines whether sample pairs are *genuine* or *imposters*. Within subgroups, performance often varies significantly from the *global* average. Thus, claims of specific error rates only hold for populations matching the validation data. We mitigate the imbalanced performances using a novel domain adaptation learning scheme on the facial features extracted using state-of-the-art neural networks. This technique balances performance, but it also boosts the overall performance. A benefit of the proposed is to preserve identity information in facial features while decreasing the demographic information they contain. The removal of demographic knowledge prevents potential future biases from being injected into decision-making. This removal improves privacy since less information is available or inferred about an individual. We explore this qualitatively; we also show quantitatively that subgroup classifiers no longer learn from the features of the proposed domain adaptation scheme. For source code and data descriptions, see <https://github.com/visionjo/facerec-bias-bfw>.

**Index Terms**—Facial recognition, Fair ML, Bias in AI, Balanced dataset, Imbalanced data problem, Domain adaptation.

## I. INTRODUCTION

THE more our society integrates with machine learning (ML), the higher the interest in bias, fairness, and the implications of using the technology [1]–[3]. Moreover, the more we depend on technology that speeds up or automates everyday tasks, the more attention concepts such as biased and unfair algorithms should receive [4], [5]. Systems deployed for sensitive tasks, such as biometrics [6] (*e.g.*, facial recognition (FR)), deserve thorough examinations. We aim to provide a test-bed for existing FR systems to report results fairly.

One typically trains an FR model on large paired data to encode faces (Fig. 1). The enrollment phase comprises feature extraction and storage, which we compare at inference time to the features of a test face. Today, models are convolutional neural networks (CNNs) trained to represent face features in N-dimensions with minimal distances between the same identity and maximum between unique identities.

The aim is to learn the optimal criterion from multiple faces from the train set - in the form of threshold (*i.e.*,  $\theta$ ) - to then

impose as a decision boundary to transform the similarity score  $s$  for a pair of unseen face to a class label (*i.e.*, *genuine* or *imposter*). Ideally, the face features of true pairs yield scores that satisfy criterion  $s \geq \theta$  [7]–[10]. Hence,  $\theta$  serves as a trade-off parameter concerning the false-positive (FP) and false-negative (FN) rates (Fig. 2).

Different sub-groups (*e.g.*, ethnicity and gender) have different distributions in the held-out validation set than the data inferred in practice. The single global threshold can favor specific demographics. The optimal threshold  $\theta$  becomes a function of demographics (Fig. 3). This problem is solvable via variable points, *i.e.*, sliding thresholds set according to demographic information [11].

The adverse effects of a global threshold are three-fold: (1) evaluation sets are typically imbalanced, so the global performance rating over-represents the demographic of some subgroups, leading to algorithms that favor the traits of those subgroup(s); (2) score ranges for genuine vary across demographics; pairs from a more popular subgroup can yield higher scores than faces of samples from underrepresented subgroups (Fig. 4); (3) the optimal scores per-subgroup vary, meaning a single, global threshold is only optimal if set and tested on a single subgroup. As shown in the signal detection model (SDM) (Fig. 4), which depicts the distributions of pair-wise scores per subgroup, show different subgroups have different optimal decision boundaries in score space (Fig. 2). Throughout this work, we use the term *global* when discussing values averaged across all demographics, which we contrast to *subgroup-specific* when referring to a demographic.

To address the imbalanced data (*i.e.*, (1)), we propose a proxy dataset, Balanced Faces In the Wild (BFW), to measure subgroup biases in FR (Fig. 5). BFW is a fair evaluation for FR systems by considering demographic-specific performances (Table I). We can now understand the performance gap in facial features from state-of-the-art (SOTA) CNNs. We then suggest a mechanism to eliminate such prejudice and level out performance ratings across demographics while improving overall accuracy. Specifically, we preserve identity information and remove demographic knowledge from the features. Thus, the lower-dimensional mappings with fewer subgroup knowledge. This feature adaptation scheme addresses items 2-3.

A byproduct of the proposed applies to problems in privacy. The learned features in the lower-dimensional space contain less knowledge of the subgroups, making it more challenging to extract the ethnicity and gender information from a face. Protecting user data is valuable, as it lessens the

J.P. Robinson ([www.jrobvision.com](http://www.jrobvision.com)) is with Vicarious Surgical, Waltham, MA. C. Qin, and Y. Fu are at the College of Engineering, Northeastern University, Boston, MA, where Robinson still was at the beginning of this effort. Y. Hann and S. Timoner are with ISM, Cambridge, MA.

Manuscript submitted ?? April 2022.

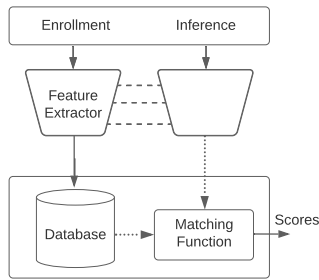


Fig. 1: **Generic FR system.** *Enrollment*: encode faces and store in a database. *Inference*: extract features from a test face and match them to those in the database to produce scores.

chance that a malicious adversary will use it in detrimental ways [12]. It is therefore essential for researchers to protect the personal attributes of the user.

The contributions of this journal extension of [11] are:

- Demonstrate a bias in CNNs with our BFW dataset. We added another attribute representing facial skin tones.
- Propose a feature learning scheme that de-biases face features and balances performances across subgroups, increasing overall performance.
- Minimize subgroup information in features – a byproduct of the proposed is the reduction of subgroup-based knowledge to address privacy concerns and avoid other potential biases.
- Provide insights with analysis of challenging samples overcome by the proposed debiasing scheme.

We now explain the organization of the paper. We review related work (Section III). Then, we go over the construction of the BFW database (Section III). Following this, we introduce the proposed method (Section IV). Then, the settings and results of the experiments are covered (Section V). Finally, we conclude and discuss the next steps (Section VI).

## II. RELATED WORK

We discuss modern-day FR systems (*i.e.*, SOTA neural network (NN)-based), the benchmark datasets, and training procedures for data-driven frameworks. The supporting data focused on balance across label types follows. Then, we describe several related works in domain adaptation. Finally, we review the problems of privacy in FR.

### A. Bias in FR

In 2014, Taigman *et al.* first proposed using a deep CNN for FR [13]. Over a half of a decade later, there has been at least one significant contribution in conventional FR each year ever since (*i.e.*, 2015 [14], 2016 [15], 2017 [8], 2018 [7], 2019 [16], 2020 [17] and 2021 [18]). Scholars provide details on advances in FR in recent surveys [19], [20]; for challenges of bias in FR see [21]. Researchers have spent significant efforts proposing problem statements and solutions to bias in FR technology [22], [23].

Some focus on characterizing performance across *soft attributes*, such as gender [24], ethnicity, age [6], or other characteristics [25]. Synthesis methods have been used to

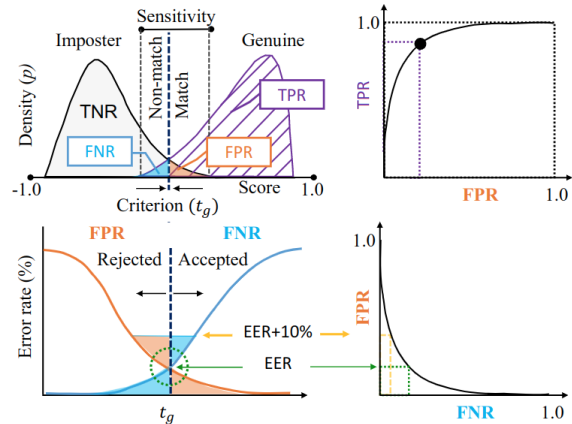


Fig. 2: **Depiction of biometrics.** The score distribution shows the sensitivity of a single threshold  $t_g$  (*top-left*). To the right of the threshold are all sample pairs predicted as positives. Plotting TPR per FPR is a common way to report FR systems (*top-right*). Equally common in FR is the trade-off between FNR and FPR (*bottom-left* and *bottom-right*).

measure bias. For example, Balakrishnan *et al.* trained a generator to manipulate latent space features in that the controlled attributes were skin tone, length of hair, and hair color [26]. Georgopoulos *et al.* generated faces across various ages to augment training data [27]. Around the same time, Muthukumar *et al.* studied the effects of color tone on gender classification by recoloring faces in images across a spectrum (*i.e.*, lighter to darker) while holding all other features constant [28]. Other recent works use knowledge distillation (*c.f.*, [29] and [30]); others form subgroups based on skin-tone [31].

Some aim to characterize the amount of bias in a system, rather than just soft attributes, whether for gender [32]–[34], ethnicity, age [35], or multiple [36]–[40]. A recent *European Conference on Computer Vision* (ECCV) challenge provided an incentive for researchers to tackle bias concerning ethnicity, gender, age, pose, and with and without sunglasses [41]. Other recent works in face recognition (FR) technology introduce additional modalities, such as profile information, to the problem of bias [42], [43]. Other questions concern the measures of biases in FR systems [32], [37], FR templates [44], score level biases [27], and biases in existing (*i.e.*, trained) models [45]. Wang *et al.* introduced a reinforcement learning-based race balanced network to find optimal margins for non-Caucasians as a Markov decision process before passing to the deep model that learns policies for an agent to select margins as an approximation of the Q-value function—it reduces variations in scattering between features across races [46]. HCI-based semi-supervised views detect bias with humans in the loop [47]. The aforementioned differs from the proposed by working in image-space, whereas we target the features extracted from existing models without retraining the original model.

Terhorst *et al.* and Cavazos *et al.* recognized the same phenomena we found in our work: the variation in the

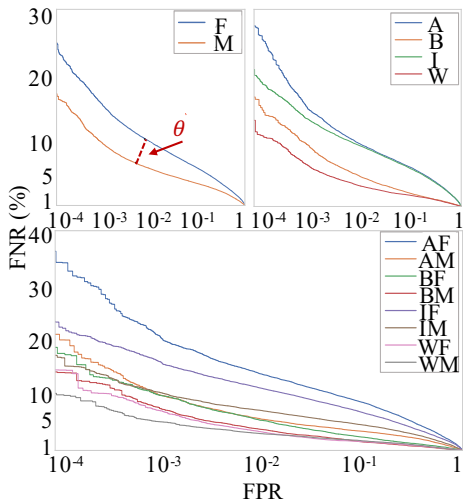


Fig. 3: **DET curves.** *Top-left:* per gender. *Top-right:* per ethnicity. *Bottom:* per subgroup (*i.e.*, combined). The dashed line shows about  $2\times$  difference in FPR for the same threshold  $\theta$ . FNR is the match error count (closer to the bottom is better).

sensitivities of scores for different demographics [48], [49]. Terhorst *et al.* propose a score normalization scheme to handle the problem of inaccurate performance ratings when comparing demographic-specific performances to the average—an issue we highlighted in [11], and which we now extend.

Khan *et al.* recently studied the limitations of face datasets with racial categories, including BFW [50]. The authors note the challenges of creating precise definitions of subgroups and measure the self-consistency of face datasets and the cross-dataset consistency. (BFW is approximately as consistent as other datasets used to measure bias.) Khan *et al.* note the challenges of racial types in science and the problems that arise without them (*e.g.*, generative models generating only Caucasian faces).

### B. Imbalanced data and data problems in FR

The impact of the quality of fairness depends on the context. There have been many proposals of various paradigms for a solution: some alter the data distribution to yield classifiers of equal performances for all classes (*i.e.*, resampling, like by under-sampling and oversampling [51]); others change the data itself (*i.e.*, algorithms that adjust classification costs). Some researchers have altered the training to reduce bias [52], [53]. Oquab *et al.* re-sampled at the image patch level [54]. Specifically, the aim was to balance foregrounds and backgrounds for object recognition. Rudd *et al.* proposed the mixed objective optimization network (MOON) architecture [55] that learns to classify attributes of faces by treating the problem as a multi-task attribute (*i.e.*, a task per attribute) to balance performances when training on data that has an imbalanced distribution across attributes. The Cluster-based Large Margin Local Embedding (CLMLE) [56] sampled in the feature-space regularized the models at the decision boundaries of underrepresented classes. Wang *et al.* changed images by masking out aspects of humans that cause

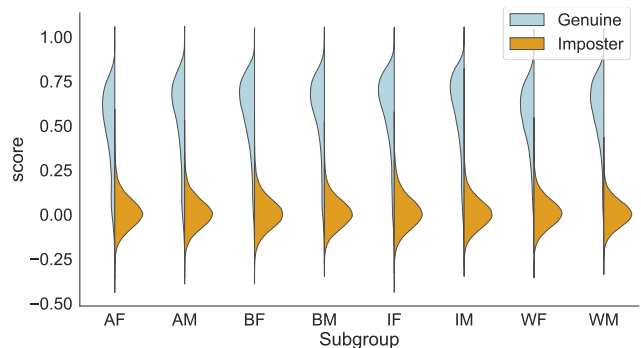


Fig. 4: **Score distributions per subgroup.** Scores of *imposters* have  $\mu \approx 0.0$  but with variations in upper percentiles; *genuine* pairs vary in mean and spread. A threshold varying across different subgroups yields a constant FPR.

“leakage” of gender information to avoid biasing a set of labels describing a scene to that of a specific gender [57]. Solutions based on the data or at the algorithmic-level are described in past reviews [58]–[60].

More specific to faces, Drozdowski *et al.* summarized that the cohorts of concern in biometrics are demographic (*e.g.*, sex, age, and race), person-specific (*e.g.*, pose or expression [61], and accessories like eye-wear or makeup), and environmental (*e.g.*, camera-model, sensor size, illumination, and occlusion) [6]. Albiero *et al.* and Gwilliam *et al.* found that balanced data sets do not necessarily yield balanced results [62], [63]. We study demographics’ effect on facial verification (FV) by assessing demographic-specific performances. Our BFW data resource allows us to analyze existing SOTA deep CNNs on different demographics (or subgroups). We provide practical insights showing that experiments often report misleading performance ratings that depend on demographics.

To match the capacity of modern-day deep models, many released large FR datasets [64]–[67]. More recently, several focused on balancing the demographics in FR data [3], [68]–[70]. Diversity in Faces (DiF) came first [70], which did not include identity labels. DiF is no longer available for download. Others released data with demographics balanced and did not include identity labels [3], [69]. Hupont *et al.* proposed DemogPairs balanced across six subgroups of 600 identities from CASIA-WebFace (CASIA-W) [71], VGG [65], and VGG2 [66]. Our BFW includes eight subgroups (*i.e.*, split the African/Indian subgroup used in DemogPairs into separate groups, Black and Indian), 800 identities, and more face samples per identity. We only used the VGG datasets and not CASIA-Web to test a broader range of models (*i.e.*, even models trained on CASIA-Web). With public resources used to train existing models, we built BFW from just VGG2 to minimize conflicts in the overlap between train and test. Table I compares our data with the others.

### C. Feature alignment / Domain adaptation (DA)

DA employs labeled data from the source domain to generalize well to the typically label-scarce target domain. Hence, a standard solution to relieve annotation costs [72]–[74]. We can roughly classify DA as the semi-supervised

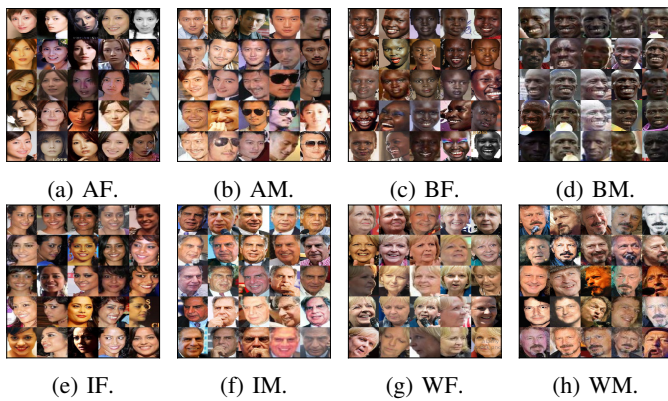


Fig. 5: **Samples of BFW.** For each subgroup, we show 25 samples for a single, randomly selected subject.

DA [74] or the unsupervised one [75] according to the access to target labels. The crucial challenge toward DA is the distribution shift of features across domains (*i.e.*, domain gap), which violates the distribution-sharing assumption of conventional machine learning problems. In our case, the domains are the subgroups (Table II).

Some Feature Alignment (FA) methods attempt to project the raw data into a shared subspace where certain feature divergence or distance confuses groups. Many developed methods following this paradigm, such as Correlation Alignment (CORAL) [76], Maximum Mean Discrepancy (MMD) [77], and Geodesic Flow Kernel (GFK) [78], [79]. Currently, adversarial domain alignment methods (*i.e.*, DANN [80], ADDA [81]) have attracted increasing attention by designing a zero-sum game between a domain classifier (*i.e.*, discriminator) and a feature generator. The discriminator could not differentiate the source and target features if it mixed the features of different domains up. More recently, learning well-clustered target features proved helpful in conditional distribution alignment. Both DIRT-T [75] and MME [74] methods applied an entropy loss on target features to group them implicitly as multiple clusters in the feature space to keep the discriminative structures through adaptation. Inspired by FA, we aim to align the score distributions of the different subgroups by adjusting the sensitivities in true scores (Fig. 4).

#### D. Protecting demographic information in FR

For reasons of privacy and protection, recent attempts remove demographic features from the raw face images [82]–[84]. These works recognized the importance of maintaining the identity information in facial features while ridding it of evidence of demographics. Our model inherently does this as part of the target, aiming for an inability to recognize subgroups. Some achieved this using adversarial learning on top of the features via a Minimax filter [85]: maximizing the attributes loss while minimizing the target task. Later on, several approached it as a minimization problem by reversing the gradient of the protected classifier. For instance, Bertran *et al.* learned a projection that maps images to an embedding space to disallow inference in gender information [86]. Similar to this, we also aim to rid the data

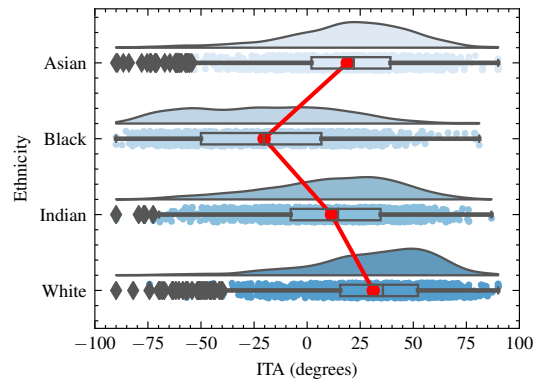


Fig. 6: **ITA values by racial group.** Smaller ITA values are darker. Mean ITA per racial category matches expectations (red line); Black is darkest, White, and Asian are lightest. Values are summarized using scattered, box, and distribution.

of demographic knowledge; however, the difference is that we learn to protect demographics in the facial features often stored in place of imagery (*i.e.*, we map from a bias to a non-bias feature space). Ray *et al.* followed the same path (*i.e.*, map image-to-feature with demographic information protected) [87]. Again, we aim to preserve a database of facial features, with no assumption that the initial model or the raw images are accessible. Besides, Wu *et al.* removed gender information from video features for action classification and, hence, their targets are human activities [88], [89]. In this work, we focus on still-image features for FR.

Wu *et al.* focused on concepts of getting rid of identity information, as seen by a task-specific ensemble of models by modifying video data in image-space [88]. For instance, by cropping out faces or the entire bodies of subjects in the video. We use a single model to change the facial features by learning a mapping to a feature space where the protected variables are unrecoverable but without compromising the performance of the FR system, which we improve. Although these existing works were motivated by privacy, they differ in ideology, methodology, and even the problem statements, data, and tasks.

Those above assumed that the facial encoding is accessible - this makes sense in reduced computations (*i.e.*, unnecessary to encode each time) and storage (*i.e.*, face features are compressed representations). However, several works aimed to hide attribute information in image space. For instance, Othman *et al.* learned to morph faces to suppress gender and preserve identity information in the image space [90]. Guo *et al.* proposed a mapping from image to noise, encrypting the image such that the encoder still decodes the identity but without the ability to determine gender by machine or human [91]. Ma *et al.* designed protocols for transferring facial features via a cascade of classifiers in their lightweight privacy-preserving adaptive boosting (AdaBoost) framework [92]. Dhar *et al.* attempt to remove the attributes information from a pre-trained CNN with the help of discriminators and an injected generator layer [93]. However, it is required to use multiple binary discriminators with the

TABLE I: **BFW features compared to related resources.** Note the balance across identity (ID), gender (G), and ethnicity (E). Compared with DemogPairs, BFW provides more samples per subject and subgroups per set. Also, BFW uses a single resource, VGG2. All the while, RFW supports a different task (*i.e.*, subgroup classification). RFW and FairFace focus on race distribution without the support of identity labels. Code available on GitHub.

| Database        |                      | Number of |         |           | Balanced Labels |   |   |
|-----------------|----------------------|-----------|---------|-----------|-----------------|---|---|
| Name            | Source               | Faces     | IDs     | Subgroups | ID              | E | G |
| RFW [3]         | MS-Celeb-1M          | ≈80,000   | ≈12,000 | 4         | ✗               | ✓ | ✗ |
| DemogPairs [68] | CASIA-W, VGG (+2)    | 10,800    | 600     | 6         | ✓               | ✓ | ✓ |
| FairFace [69]   | Flickr, Twitter, Web | 108,000   | –       | 10        | ✗               | ✓ | ✓ |
| BFW (ours) [11] | VGG2                 | 20,000    | 800     | 8         | ✓               | ✓ | ✓ |

TABLE II: **Data statistics, vocabulary, and scores for subgroups as part of our BFW data.** *Top:* Specifications of BFW and subgroup definitions. *Middle:* Number of pairs for each partition. *Bottom:* Accuracy using a global threshold  $t_g$ , the value of the optimal threshold  $t_o$ , and accuracy using  $t_o$  (bottom) per subgroup. We group columns by race and then further split them by gender. Notice that ratings are inconsistent across subgroups. Note the acronyms for the subgroups.

|                     | Asian (A)   |           | Black (B) |         | Indian (I) |         | White (W) |         | Aggregated    |
|---------------------|-------------|-----------|-----------|---------|------------|---------|-----------|---------|---------------|
|                     | Female (AF) | Male (AM) | BF        | BM      | IF         | IM      | WF        | WM      |               |
| No. Faces           | 2,500       | 2,500     | 2,500     | 2,500   | 2,500      | 2,500   | 2,500     | 2,500   | 20,000        |
| No. Subjects        | 100         | 100       | 100       | 100     | 100        | 100     | 100       | 100     | 800           |
| No. Faces / subject | 25          | 25        | 25        | 25      | 25         | 25      | 25        | 25      | 25            |
| No. Positive        | 30,000      | 30,000    | 30,000    | 30,000  | 30,000     | 30,000  | 30,000    | 30,000  | 240,000       |
| No. Negative        | 85,135      | 85,232    | 85,016    | 85,141  | 85,287     | 85,152  | 85,223    | 85,193  | 681,379       |
| Total               | 115,135     | 115,232   | 115,016   | 115,141 | 115,287    | 115,152 | 115,223   | 115,193 | 921,379       |
| Acc@ $t_g$          | 0.876       | 0.944     | 0.934     | 0.942   | 0.922      | 0.949   | 0.916     | 0.918   | 0.925±0.022   |
| $t_o$               | 0.235       | 0.274     | 0.267     | 0.254   | 0.299      | 0.295   | 0.242     | 0.222   | 0.261±0.025   |
| Acc@ $t_o$          | 0.916       | 0.964     | 0.955     | 0.971   | 0.933      | 0.958   | 0.969     | 0.973   | 0.955 ± 0.018 |

correspondence with each attribute. Instead, we have applied a single multi-class classifier to fulfill such an object, ensuring dense computation and improving model efficiency.

### III. BALANCED FACES IN THE WILD (BFW)

BFW provides balanced data across ethnicity (*i.e.*, Asian (A), Black (B), Indian (I), and White (W)) and gender (*i.e.*, Female (F) and Male (M))—eight demographics referred to as subgroups (Fig. 5). As in Table I, BFW has an equal number of subjects per subgroup (*i.e.*, 100 subjects per subgroup) and faces per subject (*i.e.*, 25 faces per subject). Note that the key difference between BFW and DemogPairs is in the additional attributes and the increase in overall labeled data; the differences between RFW and FairFace are in the identity labels and distributions (Table II).

We built BFW with VGG2 [66] by using classifiers on the list of names and then the corresponding face data. Specifically, we ran a name-ethnicity classifier [94] to generate the initial list of subject proposals. Then, the corresponding faces with ethnicity [95] and gender [96] classifiers further refined the list. Next, we manually validated, keeping only those that were genuine members of the respective subgroup. We then limited faces for each subject to 25 faces selected at random. Thus, BFW costs minimal human input, having generated the proposal lists by automatic machinery.

In summary, four experts in FR manually validated all the data: first, the validation of individuals per subgroup was conducted (*i.e.*, inspect that all subjects belong to the assigned

subgroups), and then the faces of the individual (*i.e.*, verify that each face instance belongs to the identity). We only kept the subjects and samples that all four annotators marked as correct. We refer the reader to our conference paper for more details [11].

We determined the subgroups of BFW based on physical features most common amongst the respective subgroup [11]. We can regard this as multiple domains because of the feature distribution mismatch across these subgroups. However, the assumption is that a discrete label that can describe an individual is imprecise. The assumption allows for a finer-grain analysis of the subgroup and is a step in the right direction. Thus, we refute any claim that our efforts here are the ultimate solution; the data and proposed machinery are merely an attempt to establish a foundation for future work to extend. The two genders for the four ethnic groups make up the eight subgroups of the BFW dataset (Fig. 5). Formally put, the tasks addressed have labels for gender  $l^g \in \{F, M\}$  and ethnicity  $l^e \in \{A, B, I, W\}$ , where the  $K$  subgroups (*i.e.*, demographics) are then  $K = |l^g| * |l^e| = 8$ .

#### A. The data subgroups

Kärkkäinen *et al.* note that the human race is determined by physical attributes, while ethnicity is cultural-based [69]. Still, people often use race and ethnicity interchangeably. We refer to the U.S. Census Bureau to choose subgroups. Such labels are oversimplified [98] and are not precisely defined

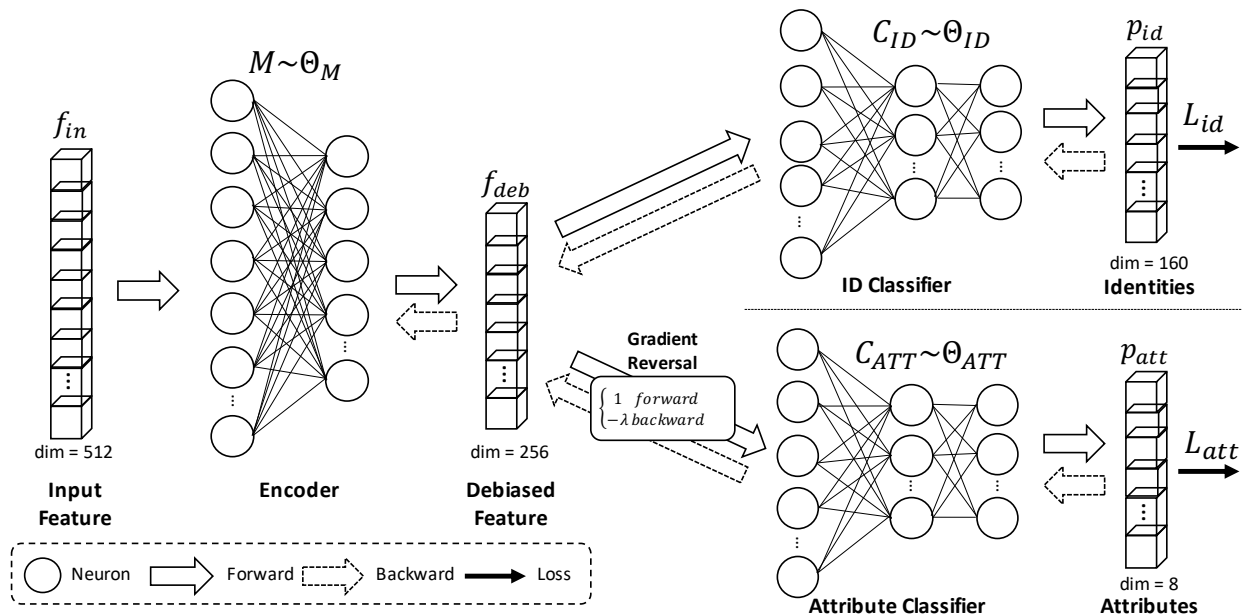


Fig. 7: **Debiasing framework.** The framework used to learn a projection that casts facial features to a space that (1) preserves identity information (*i.e.*,  $C_{ID}$ ) and (2) removes the knowledge of subgroup (*i.e.*,  $C_{ATT}$ ). The benefits are two-fold: verifying pairs of faces fairly across attributes and an inability to classify attributes for privacy and safety purposes. Note that the *gradient reversal* [97] flips the sign of the error backpropagated from  $C_{ATT}$  to  $M$  by scalar  $\lambda$  during training.

[50]. With those limitations, the categories can show value for sub-group analysis of bias in computer vision [11].

Dermatologists diagnose risks of sun exposure by manual inspection of the tone of a subject’s skin with a label called the Fitzpatrick skin type (FST). Because of the need for manual review by multiple experts, it can be challenging to collect such data. Merler *et al.* proposed a digital image processing scheme to characterize the skin tones of faces in their dataset, Diversity in Faces (DiF) [99]. The authors referenced an earlier study that revealed a correlation between the melanin index (MI), a measure objectively measured by reflectance spectrophotometry [100], and the individual typology angle (ITA): a practical measure to categorize skin tones, as the FST can be determined digitally. ITA is calculated from pixels in CIE-Lab color-space as follows:

$$\text{ITA} = \arctan\left(\frac{L - 50}{b}\right) \times \frac{180^\circ}{\pi}, \quad (1)$$

where larger lightness  $L$  and smaller blue-yellow  $b$  yield larger ITAs. We proceed following [99] (and perhaps less like Kinyanjui *et al.* [101]). We mask out target regions of the skin. However, instead of splitting face into areas based on detected landmarks, we segment faces, masking out all but the flat areas to avoid shadowing (*i.e.*, omitting the nose, eyes, mouth, and hair).<sup>1</sup> With the pixels transformed from RGB to CIE-Lab, we removed  $L$  and  $b$  values more than one standard deviation of the respective mean for that face. We further mitigated concerns of outlier pixels by smoothing them out via a mean filter. Finally, the mean of pixel-wise ITA values (*i.e.*, Eq. 1) was calculated for a face.

Fig. 6 shows the distribution of all ITA values. The values line up within expectation: the smaller the ITA (in degrees), the darker the skin tone. Notice that the left tail of the Black, Indian, Asian, and White go from most dense to the most scarce. Furthermore, the mean (*i.e.*, vertical line in the figure) shifts right for the lighter-toned skin subgroups. There is a significant spread in values within racial groups, which is partly due to the varied lighting conditions.

#### IV. METHODOLOGY

To discuss the bias and privacy concerns of facial verification (FV) systems, we first introduce the problem. Specifically, we review the problem statement, the supporting facial image dataset, and the proposed framework. We aimed to preserve identity information, balance the sensitivities of features for the different demographics (*i.e.*, subgroups), and remove evidence of the subgroups from the facial encoding – the typical representation available for use cases.

##### A. Problem statement

FV systems decide based on the likeliness that a pair of faces are of the same identity. The core procedure of verification systems is often similar to the FR employed for various applications. Specifically, we train a Convolutional Neural Network (CNN) on a closed set of identities and later use it to encode faces (*i.e.*, map face images to features). We then compared the features in closeness to produce a single score—often via cosine similarity in FR [102]. It is imperative to learn the optimal score threshold separating valid from false pairs. The threshold is the decision boundary in score space, *i.e.*, the *matching function*.

<sup>1</sup>[https://github.com/shaoanlu/face\\_toolbox\\_keras](https://github.com/shaoanlu/face_toolbox_keras)

1) *The matching function*: A real-valued similarity score  $R$  assumes a discrete label of  $Y = 1$  for *genuine* pairs (*i.e.*, a true-match) or  $Y = 0$  for *imposter* (*i.e.*, untrue-match). We map the actual real number to a discrete label by  $\hat{Y} = \mathbb{I}\{R > \theta\}$  for some pre-defined threshold  $\theta$ . We can express the aforementioned as *matcher*  $d$  operating as

$$f_{boolean}(\vec{x}_i, \vec{x}_j) = d(\vec{x}_i, \vec{x}_j) > \theta, \quad (2)$$

where the face features in  $\vec{x}$  being the  $i^{th}$  and  $j^{th}$  sample—a conventional scheme in the FR research communities [103]. We use cosine similarity as the *matcher* in Eq. 2, which produces a score in closeness for the  $i^{th}$  and  $j^{th}$  faces (*i.e.*,  $l^{th}$  face pair) by  $d(\vec{x}_i, \vec{x}_j) = s_l = \frac{f_i \cdot f_j}{\|f_i\|_2 \|f_j\|_2}$ . The decision boundary formed by the threshold  $\theta$  controls the level of *acceptance* and *rejection*. Thus,  $\theta$  inherits a trade-off between sensitivity and specificity. The value of  $\theta$  depends on the purpose of the system. For instance, in security there is a need for higher sensitivity (*i.e.*, smaller  $\theta$ ). Specifically, the trade-off involves FNR that attempts to pass but falsely rejects—a Type 1 Error. Mathematically, it relates by

$$\text{FNR} = \frac{\text{FN}}{P} = \frac{\text{FN}}{\text{FN} + \text{TP}} = 1 - \text{TPR} = 1 - \frac{\text{TP}}{\text{FN} + \text{TP}},$$

with positive counts  $P$ .

The other error type contributes to the FPR, the Type II Error, which is when an *imposter* falsely passes:

$$\text{FPR} = \frac{\text{FP}}{N} = \frac{\text{FP}}{\text{FP} + \text{TN}} = 1 - \text{TNR} = 1 - \frac{\text{TN}}{\text{FP} + \text{TN}},$$

where the number of negatives is  $N$ , with metrics true-negative (TN), false-positive (FP), true-negative rate (TNR), and FPR. A *matching* function is a module typically characterized using the listed metrics (Fig. 1). The geometric relationships of the metrics related to the score distributions and the choice of threshold shows the trade-offs in error rates (Fig. 2).

The hyper-parameter  $\theta$  determines the desired error rate on held-out validation, specific to the use case. Researchers tend to set it for top performance. Some analyze  $\theta$  as a range of values, for a complete characterization is often obtainable with evaluation curves that inherently show performance trade-offs. However, the held-out validation and test sets typically share data distributions as a single source partitioned into subsets (*i.e.*, train, validation, test). Regardless, we transfer the decision boundary in score space that maximizes the performance to the pin-point (*i.e.*, 1D) decision boundary. The floating-point value spans  $[0, 1]$ .

2) *Feature alignment*: The tuple  $\mathcal{D} = \{(\mathbf{x}_i, y_i) \in \mathcal{X} \times \mathcal{Y}\}_{i=1}^N$  represents domain  $\mathcal{D}$ , with  $\mathcal{X}$  and  $\mathcal{Y}$  representing the input feature space and output label space, respectively. FR algorithms aim to learn a mapping function (*i.e.*, a hypothesis):  $\eta: \mathcal{X} \rightarrow \mathcal{Y}$ , assigning vectors with a semantic identity label.

Mathematically, we denote the labeled source domain  $\mathcal{D}_S$  and the unlabeled target domain  $\mathcal{D}_T$  as  $\mathcal{D}_S = \{(\mathbf{x}_i^s, y_i^s) \in \mathcal{X}_S \times \mathcal{Y}_S\}_{i=1}^{N_S}$  and  $\mathcal{D}_T = \{\mathbf{x}_i^t \in \mathcal{X}_T\}_{i=1}^{N_T}$  with the sample count  $N_S = |\mathcal{D}_S|$  and  $N_T = |\mathcal{D}_T|$  corresponding to the  $i$ -th sample (*i.e.*,  $\mathbf{x}_i \in \mathbb{R}^d$ ) and label (*i.e.*,  $y_i \in \{1, \dots, K\}$ ).  $\mathcal{D}_S$  and  $\mathcal{D}_T$  are further defined by tasks  $\mathcal{T}_S$  and  $\mathcal{T}_T$ , which show the exact

label type(s) and the specific  $K$  classes of interest. The goal is to learn an objective  $\eta_S: \mathcal{X}_S \rightarrow \mathcal{Y}_S$ , then transfer to target  $\mathcal{D}_T$  for  $\mathcal{T}_T$ . By this, we leverage knowledge from both  $\mathcal{D}_S$  for  $\mathcal{D}_T$  to get  $\eta_T$ . Since either domain has different marginal distributions (*i.e.*,  $p(\mathbf{x}^s) \neq p(\mathbf{x}^t)$ ) and distinct conditional distributions (*i.e.*,  $p(y^t|\mathbf{x}^s) \neq p(y^t|\mathbf{x}^t)$ ) a model trained on the labeled source usually performs poorly on the unlabeled target. A typical solution to such a domain gap is to learn a model  $f$  that aligns the features in a shared subspace by  $p(f(\mathbf{x}^s)) \approx p(f(\mathbf{x}^t))$ .

## B. Proposed framework

We used both identity and subgroup labels for the two objectives of the proposed framework (Fig. 7). Specifically,  $\mathcal{D} = \{\mathbf{x}_i, y_i^{id}, y_i^{att}\}_{i=1}^N$ , where  $\mathbf{x} \in \mathbb{R}^d$ ,  $y^{id} \in \{1, \dots, I\}$  and  $y^{att} \in \{1, \dots, K\}$ . Hence, we aim to learn a mapping  $\mathbf{f}_{deb} = M(\mathbf{x}, \Theta_M)$  to a lower-dimensional space  $\mathbf{f}_{deb} \in \mathbb{R}^{d/2}$  that preserves the identity information of the target. We call this the identity loss  $\mathcal{L}_{ID}$ . Then, we learn to do so without subgroup information, which we call the attribute (or subgroup) loss  $\mathcal{L}_{ATT}$ . The total loss (*i.e.*, the final objective  $\mathcal{L} = \mathcal{L}_{ID} + \mathcal{L}_{ATT}$ ) is the sum of all losses.

$$\mathcal{L}_{ID} = -\frac{1}{N} \sum_{i=1}^N \sum_{k=1}^I \mathbf{1}_{[k=y_i^{id}]} \log(p(y = y_i^{id}|\mathbf{x}_i)), \quad (3)$$

$$\mathcal{L}_{ATT} = -\frac{1}{N} \sum_{i=1}^N \sum_{k=1}^K \mathbf{1}_{[k=y_i^{att}]} \log(p(y = y_i^{att}|\mathbf{x}_i)), \quad (4)$$

where  $p(y = y_i^{id}|\mathbf{x}_i)$  and  $p(y = y_i^{att}|\mathbf{x}_i)$  represent the softmax conditional probability of its identity and attribute.

We added  $\mathcal{L}_{ATT}$  to debias the features to remove variation in scores previously handled with a variable threshold. Further, a byproduct is these features that preserve identity information without knowledge of subgroup—a critical concern in the privacy and protection of biometric data.

There are three groups of parameters (*i.e.*,  $\Theta_M$ ,  $\Theta_{ID}$ , and  $\Theta_{ATT}$ ) optimized by the objective (Fig. 7). Both classifiers, the identity  $\mathcal{C}_{ID}$  and the attribute  $\mathcal{C}_{ATT}$ , are used to find a feature space that remains accurate to identity and not for subgroup by minimizing the empirical risk of  $\mathcal{L}_{ID}$  and  $\mathcal{L}_{ATT}$ :

$$\Theta_{ID}^* = \arg \min_{\Theta_{ID}} \mathcal{L}_{ID}, \quad (5)$$

$$\Theta_{ATT}^* = \arg \min_{\Theta_{ATT}} \mathcal{L}_{ATT}. \quad (6)$$

It is important to note that  $\mathcal{L}_{ATT}$  aims to be incorrect (*i.e.*, learn a mapping that contains no knowledge of the subgroup). Thus, a gradient reversal layer [97] that acts as the identity during the forward pass, while inverting the sign of the gradient back-propagated with a scalar  $\lambda$  as the adversarial loss during training:

$$\Theta_M^* = \arg \min_{\Theta_M} -\lambda \mathcal{L}_{ATT} + \mathcal{L}_{ID}. \quad (7)$$

Although the proposed learning scheme is simple, it proved effective for both objectives we seek to solve. Next, we illustrate the effectiveness of the results and provide analysis.

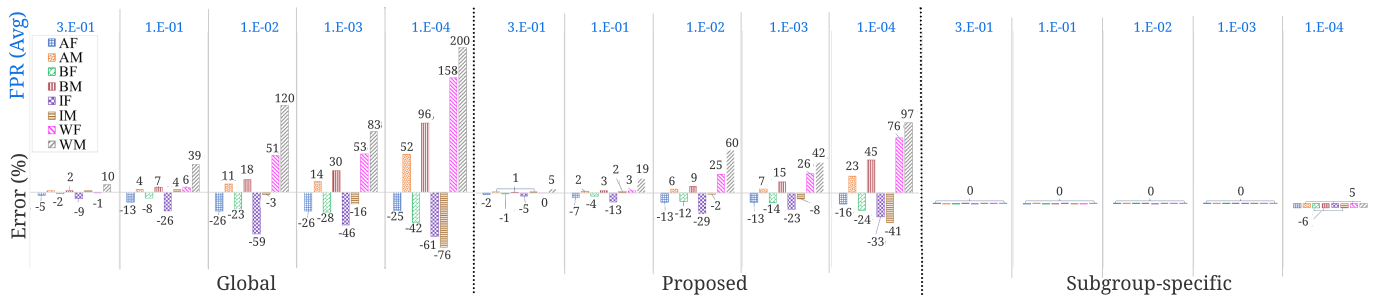


Fig. 8: **The percent differences from the global FPR across subgroups.** *Left:* global threshold ( $t_g$ ) yields an FPR that spans up to 200% of the intended (*i.e.*, WM for  $1e-4$ ); the F subgroups perform worse than average, while M’s overshoot the average performances besides IM at  $FPR=1e-4$ . *Right:* Subgroup-specific thresholds  $t_o$  reduces the difference closer to zero. Furthermore, the proposed method (*middle*), which does not assume knowledge of attribute information at inference like for  $t_o$ , clearly mitigates the issue of the inconsistencies in the *global FPR* versus *subgroup-specific FPR*. Similar to the results in Fig. 9, the variations are nearly halved: the percent difference for subgroups is more balanced using the features adapted with our approach versus the baseline.

V. EXPERIMENTS

We include two sets of experiments to show the effectiveness of the proposed using our balanced BFW [11]. First, we evaluate verification performance. Specifically, we compare the *global* results compared to the *subgroup specific* results. Then, for the privacy-preserving claim, we compare the performance of models trained on top of debiased features  $f_{deb}$  with those of the original features  $f_{in}$ . For each, we present the problem statement, metrics and settings, and analysis. Finally, we do an ablation study to show the performance of the renowned LFW benchmark [103].

A. Common settings

We employed Arcface (*i.e.*, ResNet-34) as the baseline (*i.e.*,  $f_{in}$ ) [9].<sup>2</sup> MS1M [64] was the train set, with about 5.8M faces for 85k subjects. We prepared the faces using MTCNN [104] to detect five facial landmarks. We then applied a similarity transformation to align the face by the five detected landmarks, from which we cropped and resized each to  $96 \times 112$ . The RGB (*i.e.*, pixel values of  $[0, 255]$ ) were normalized by centering about 0 (*i.e.*, subtracting 127.5) and then standardizing (*i.e.*, dividing by 128); features were later L2 normalized [105]. The batch size was 200, and an SGD optimizer with a momentum of 0.9, weight decay  $5e-4$ , and learning rate started at 0.1 and factored by 10 two times when the error leveled. We chose these settings based on Arcface being among the best performing FR deep models to date. It has become a popular choice for an *off-the-shelf* option for face recognition technology and applications.

We used our BFW dataset (Section III): the debias and privacy-based experiments use the pre-defined five-folds<sup>3</sup>; the ablation study on LFW uses all of BFW to train M (Fig. 7). As mentioned, we built BFW using data of VGG2, and there is no overlap between CASIA-Webface and LFW used to train the face encoder and for the ablation, respectfully.

B. Debias experiment

The percent error is a typical metric for FR systems - whether to a customer or prospective staff. Specialized curves, confusion matrices, and other metrics are not always the best way to communicate system performances to nontechnical audiences. Specifically, global ratings (*e.g.*, overall average) are easier to comprehend in practice. A prime example is to share the error rate per number correctly predicted (*e.g.*, falsely classify one in ten thousand). For instance, claiming that a system predicts an FP in 1 of 10,000 predictions. However, such an approximation can be hazardous, for it is inherently misleading. To show this, we ask the following questions. *Does this hold for different demographics? Does this rating depend on the faces - does it carry for all males and females?* Thus, setting our system according to the desired false-positive rate (FPR) is fair regardless of the demographics (*i.e.*, subgroups) of the population.

The questions above were central to our previous work [11]. We found the answer to these questions to be clear - *No, the reported FPR is not true when analyzed per subgroup.* When comparing the FPR values (*i.e.*, the *subgroup-specific-to-the-global*), the values drastically deviate from the *global average* when the score threshold is fixed for all subgroups. Demographic-specific thresholds, meaning an assumption that demographic information is known prior, proved to mitigate the problem. However, prior knowledge of demographic, although plausible (*e.g.*, identifying a known subject on a *blacklist*), a strong assumption limits the practical uses for which it could be deployed. To extend our prior work, we propose a debiasing scheme to reduce the differences between the *global* and *subgroup-specific*. We set out to claim *subgroup-specific* error rates to be fair across all involved demographics.

1) *Metrics and settings:* TPR and FPR are used to examine the trade-off in the confusions dependent on the choice of threshold discussed earlier. Specifically, we look at *subgroup-specific* TPR scores at the desired FPR (Fig. 9). We compute the following metric, the percent difference of the *global*

<sup>2</sup><https://github.com/deepinsight/insightface>  
<sup>3</sup><https://github.com/visionjofacerec-bias-bfw>



| FPR  | 0.3   | 0.1   | 0.01  | 0.001 | 0.0001 |                   |
|------|-------|-------|-------|-------|--------|-------------------|
| AF   | 0.990 | 0.867 | 0.516 | 0.470 | 0.465  | Subgroup-Specific |
|      | 0.996 | 0.874 | 0.521 | 0.475 | 0.470  | Proposed          |
|      | 1.000 | 0.882 | 0.524 | 0.478 | 0.474  | Global            |
| AM   | 0.994 | 0.883 | 0.529 | 0.482 | 0.477  |                   |
|      | 0.996 | 0.886 | 0.531 | 0.484 | 0.479  |                   |
|      | 1.000 | 0.890 | 0.533 | 0.486 | 0.482  |                   |
| BF   | 0.991 | 0.870 | 0.524 | 0.479 | 0.473  |                   |
|      | 0.995 | 0.875 | 0.527 | 0.481 | 0.476  |                   |
|      | 1.000 | 0.879 | 0.530 | 0.484 | 0.480  |                   |
| BM   | 0.992 | 0.881 | 0.526 | 0.480 | 0.474  |                   |
|      | 0.995 | 0.886 | 0.529 | 0.483 | 0.478  |                   |
|      | 1.000 | 0.891 | 0.532 | 0.485 | 0.480  |                   |
| IF   | 0.996 | 0.881 | 0.532 | 0.486 | 0.481  |                   |
|      | 0.998 | 0.883 | 0.533 | 0.487 | 0.483  |                   |
|      | 1.000 | 0.884 | 0.534 | 0.488 | 0.484  |                   |
| IM   | 0.997 | 0.895 | 0.533 | 0.485 | 0.479  |                   |
|      | 0.998 | 0.897 | 0.534 | 0.486 | 0.480  |                   |
|      | 1.000 | 0.898 | 0.535 | 0.486 | 0.481  |                   |
| WF   | 0.988 | 0.878 | 0.517 | 0.469 | 0.464  |                   |
|      | 0.992 | 0.884 | 0.522 | 0.472 | 0.468  |                   |
|      | 1.000 | 0.894 | 0.526 | 0.478 | 0.474  |                   |
| WM   | 0.989 | 0.896 | 0.527 | 0.476 | 0.470  |                   |
|      | 0.996 | 0.901 | 0.530 | 0.479 | 0.474  |                   |
|      | 1.000 | 0.910 | 0.535 | 0.483 | 0.478  |                   |
| Avg. | 0.992 | 0.881 | 0.526 | 0.478 | 0.473  |                   |
|      | 0.998 | 0.886 | 0.528 | 0.481 | 0.476  |                   |
|      | 1.000 | 0.891 | 0.531 | 0.483 | 0.479  |                   |

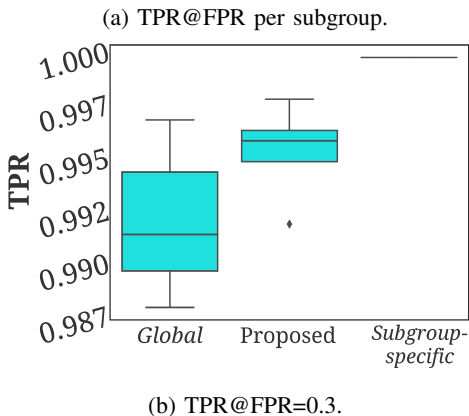


Fig. 9: **TPR at FPR.** (9a) TPR scores for global thresholds with the baseline and proposed and *subgroup-specific* baseline: higher is better. Comparing the standard deviations of the *global* to the *subgroup-specific* scores - the proposed debiasing transformation with the global threshold rather than the impractical per-subgroup thresholds. (9b) A smaller range and a boost in performance are shown in the figure below, comparing the proposed (middle) to the baseline (left).

and *subgroup-specific* FPR values (*i.e.*, an average score is targeted) at a threshold  $l$ . So we ask, *how well do the different subgroups compare to the average?* Specifically,

$$\% \text{ Error}(l) = \left( \frac{\text{FPR}(l)_{\text{subgroup}} - \text{FPR}(l)_{\text{global}}}{\text{FPR}(l)_{\text{subgroup}}} \right) * 100\% \quad (8)$$

The *global results* are the results averaged across subgroups. Then, the *subgroup-specific results*, which differ meaningfully from the mean result (*i.e.*, the global results), are analyzed independently per subgroup. Hence, there is a gap between

*global* and *subgroup-specific*, which we show in Fig. 8 using the percent error (*i.e.*,  $100\% * (\text{subgroup} - \text{global})/\text{global}$ ). Note that the percent error takes on negative scores when ( $\text{global} > \text{subgroup}$ ), meaning *subgroup-specific* are inferior.

2) *Analysis:* The proposed balance results and significantly boosts the TPR at FPR. The percent difference between *global* and *subgroup-specific* FPR scores leads to a fairer representation, especially at high FAR. Fig. 7 demonstrates the spread of scores for the various subgroups using the baseline, the proposed, and the optimal threshold at 0.3 FPR. Note that the standard deviation of TAR using the baseline approach is high, which we mitigate using the proposed scheme. The proposed has thus boosted performance: improved the overall rating, and reduced the variances.

We can interpret Fig. 8 as a practical use case. The *global* FPR implies that the system has its threshold set to yield a measure depicting the number of true-positive (TP) a verification system reports on average before making an error (*i.e.*, the number of TP before an FP is expected). The far-right (*i.e.*,  $1e-4$ ) claims that 1 in 10,000 is incorrectly matched. Again, a predetermined FPR for a verification system is set via a trade-off threshold value (*i.e.*,  $\theta$ ) that controls the level of sensitivity: decreasing the score threshold increases the FPR (Fig. 2). Fig. 8 then shows the difference between the *global* and *subgroup-specific* on the subgroup level for a set of faces with equal representation for all subgroups.

The baseline shows a 200% increase for WM at a *global* FPR of  $1e-4$ , meaning the *global* expects an FP per 10,000 TP, while the *subgroup-specific* performance doubles this (*i.e.*, all WM expect an FP per 20,000 TP).

The direction (*i.e.*,  $\pm$ ) represents whether the difference is an improvement. A negative %-difference shows a drop in performance compared to the *global result*. For instance, AF with a -25% difference for the baseline at an overall average FPR of 1 in 10,000 implies that if the population of samples comprises only AF subjects, then the FPR for the chosen  $\theta$  for the claim of 1 in 10,000 would be 1 in 7,500. A consumer expecting a FPR would only match this value when the sample population has the same distribution in samples per subgroup as that of the validation data for which  $\theta$  was found.

We can remove the percent difference via an optimal threshold. However, the assumption that subgroup-specific thresholds can be determined from validation sets that are separated by subgroup. Also, the optimal solution assumes prior knowledge of the subgroup to which the sample of interest belongs at test time. Although the method was proof in principle, both of the assumptions are impractical for most use-cases. Hence, the proposed feature transformations reduce the percent differences from the original features (*i.e.*, the baseline). The proposed and the optimal are the middle and right plots, respectively (Fig. 8).

Fig. 10 shows several hard positives and negatives that were incorrectly matched by the baseline but correctly identified by the proposed. These samples had scores closest to the global threshold (*i.e.*, score boundary). Notice the quality of at least one face per pair is low-resolution; extreme pose differences between faces of each pair also are common. The proposed scheme overcomes these challenges - mitigating bias boosts



Fig. 10: **Sample pairs.** Hard negatives (a) and positives (b) that the baseline got wrong, while the proposed got correct.

results and there displayed are several of the pairs that went from falsely being rejected to correctly being accepted.

C. Privacy-preserving experiment

We aim to preserve identity information while debiasing the facial features, as shown in the prior experiment. To do this, we use a reverse gradient when training the subgroup branch to force the process to penalize when the subgroup classifier is correct. Another benefit of the proposed debiasing scheme is that it rids the facial features of demographic information. This is of interest in problems of privacy and protection. Ideally, face features, which often are the only representation of face information available at the system level, will not include attribute information, like gender or ethnicity. Hence, by prohibiting subgroup classifiers from learning we reduce demographic information in the features.

We train a multi-layered perceptron (MLP) to classify subgroups on top of the features to show the extent to which the subgroup information was removed. We can then measure the amount of information present in the face representation [37].

The MLP implemented in Keras comprises three fully connected ( $f_c$ ) layers (i.e., sizes 512, 512, and 256) and the output  $f_c$  layer (i.e., size 8, one per subgroup). The first three layers were separated by ReLU activation and dropout [106] (i.e., probability of 0.5), while only dropout (again, 0.5) was placed prior to the output softmax layer. A categorical cross-entropy loss with Adam [107] set with a learning rate of 1e-3 was used to train.

1) *Metrics and settings:* We examine the overall accuracy of the subgroup classifiers via a confusion matrix. Specifically, we will look at how often each subgroup was predicted correctly and, when incorrect, the percentage it was mistaken for the others. The confusion was generated by averaging across the five folds. We then used the top performing threshold from the training folds on the test fold for all subgroup classifiers.

|    |      |      |      |      |      |      |      |      |
|----|------|------|------|------|------|------|------|------|
| AF | 92.7 | 7.0  | 0.0  | 0.0  | 0.1  | 0.0  | 0.2  | 0.0  |
| AM | 1.6  | 97.4 | 0.1  | 0.1  | 0.0  | 0.2  | 0.0  | 0.7  |
| BF | 0.8  | 0.0  | 92.4 | 2.8  | 0.9  | 0.0  | 3.0  | 0.0  |
| BM | 0.0  | 0.0  | 2.0  | 96.2 | 0.0  | 1.6  | 0.0  | 0.2  |
| IF | 0.9  | 0.0  | 3.0  | 0.0  | 93.5 | 0.4  | 2.2  | 0.0  |
| IM | 0.0  | 3.6  | 0.0  | 0.8  | 2.0  | 90.2 | 0.0  | 3.3  |
| WF | 0.4  | 0.4  | 0.8  | 0.0  | 0.4  | 0.0  | 97.0 | 1.1  |
| WM | 0.0  | 4.6  | 0.0  | 0.1  | 0.3  | 8.6  | 1.6  | 84.8 |

|    |      |      |      |      |      |      |      |      |
|----|------|------|------|------|------|------|------|------|
| AF | 85.2 | 8.8  | 1.1  | 0.3  | 1.7  | 0.6  | 1.5  | 1.0  |
| AM | 10.2 | 73.0 | 3.1  | 1.2  | 1.6  | 3.8  | 4.6  | 2.6  |
| BF | 3.5  | 3.8  | 64.4 | 11.4 | 5.4  | 3.2  | 6.5  | 1.8  |
| BM | 1.5  | 2.1  | 13.3 | 66.8 | 4.5  | 5.7  | 4.0  | 2.1  |
| IF | 2.2  | 2.3  | 4.6  | 5.7  | 64.9 | 13.9 | 4.2  | 2.2  |
| IM | 1.7  | 3.7  | 1.4  | 5.4  | 9.9  | 58.9 | 8.4  | 10.6 |
| WF | 1.4  | 4.5  | 5.2  | 7.9  | 5.8  | 11.7 | 54.7 | 8.8  |
| WM | 10.4 | 5.4  | 6.1  | 6.0  | 7.9  | 17.1 | 15.4 | 31.7 |

AF AM BF BM IF IM WF WM

Fig. 11: **Subgroup confusion matrix.** Comparison of accuracy in classifying and misclassifying the subgroups. Notice the bottom performs significantly worse than the top.

Also, we measure precision and recall. Precision is defined as  $P(l) = \frac{TP}{TP+FP}$ , which we average across subgroups  $l \in L$ . The recall R, is computed as  $R(l) = \frac{TP}{TP+FN}$ . This complements the confusion by allowing the specificity and sensitivity of the subgroups also to be examined. There are inherent trade-offs between P and R. This motivates the  $F_1$ -score [108], as the harmonic mean of P and R,  $F_1 = 2 * \frac{P * R}{P + R}$ .

2) *Analysis:* We showed the preservation of identity knowledge (Fig. 9), and now we show the other benefits of privacy. The results confirm that the privacy-preserving claim is accurate, leading to a 30% drop in predicting gender and ethnicity from the features (Table III). Hence, the predictive power of all subgroups dropped significantly. The decrease in performance suffices to claim that the predictions are now unreliable. Interestingly, it hindered the subgroups for which the baseline favored the most from the debias scheme. WM and WF drop the most, while the AM and AF drop the least. The same trends in confusion propagate from the baseline to the proposed results (e.g., WM mostly confuses IM initially and then again with the proposed). The same holds for cases of different sex.

TABLE III: **Subgroup classification results.** The baseline and proposed are on the left and right columns, respectively. Note that the columns on the right have lower scores as intended.

|      | Precision |       | Recall |       | F1    |       |
|------|-----------|-------|--------|-------|-------|-------|
| AF   | 0.962     | 0.734 | 0.927  | 0.852 | 0.943 | 0.788 |
| AM   | 0.864     | 0.707 | 0.974  | 0.730 | 0.915 | 0.717 |
| BF   | 0.940     | 0.655 | 0.924  | 0.644 | 0.932 | 0.647 |
| BM   | 0.961     | 0.644 | 0.962  | 0.668 | 0.961 | 0.653 |
| IF   | 0.961     | 0.641 | 0.935  | 0.649 | 0.948 | 0.644 |
| IM   | 0.898     | 0.519 | 0.902  | 0.589 | 0.898 | 0.550 |
| WF   | 0.934     | 0.554 | 0.970  | 0.547 | 0.951 | 0.549 |
| WM   | 0.943     | 0.524 | 0.848  | 0.317 | 0.892 | 0.392 |
| Avg. | 0.933     | 0.622 | 0.930  | 0.624 | 0.930 | 0.617 |

Next, we examine the confusion for the different subgroups before and after debiasing the face features (Fig. 11). As established, the baseline contains more subgroup knowledge—a model can learn on top. When trained and evaluated on BFW, the baseline performs best on F subgroups, which differs from the norm, where M is most of the data. The WM is inferior in performance to all subgroups in either case.

#### D. The privacy model

To check the effectiveness of the proposed, we train M on the BFW dataset and deploy it on the well-known LFW benchmark. We note that the training dataset we employ is significantly smaller than that used by SOTA networks trained to achieve high performance on LFW, employing the MS1MV2 dataset, which contains 5.8M images of 85k identities. Even though we initialize our network starting with features learned on MS1MV2, we train on a small dataset of 20k images of 800 subjects, two orders of magnitude smaller. The current SOTA with 99.8% verification accuracy, while the proposed scheme reaches its best score of 95.2% after five epochs before dropping off and then leveling out around 81% (Fig. 12). The unbalanced data hinders the benefits of privacy and debiasing (*i.e.*, LFW comprises about 85% WM). Furthermore, we optimized M by choosing the epoch with the best performance before the drop-off. Future steps could improve the proposed when transferring to unbalanced sets to detect the optimal settings.

## VI. CONCLUSION AND FUTURE WORK

We show a bias for subgroups in FR caused by the selection of a single threshold. Previously, we proposed a *subgroup-specific* threshold for when knowledge of subgroup information is accessible prior. Inspired by feature alignment and domain adaptation, we propose to mitigate the bias present in FR by learning a lower-dimensional mapping that preserves identity and removes the knowledge of the subgroups from the features. With the proposed, the performance across subgroups not only balances but also boosts the overall accuracy. We reduce the difference between *subgroup-specific performance* and *global performance* across subgroups using a single threshold. The resulting features hold reduced knowledge of subgroups, increasing privacy concerning demographics (*i.e.*,

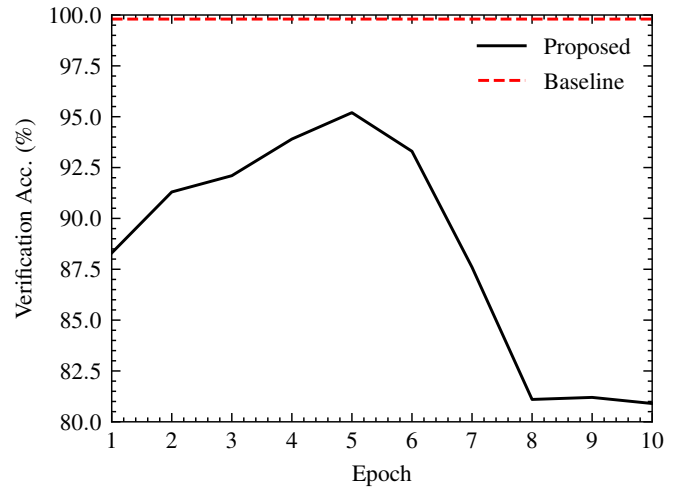


Fig. 12: **Accuracy on LFW.** The proposed nears the baseline performance of 99.8%, with its top score of 95.2%. By this, privacy is preserved with limited accuracy compromised.

gender and ethnicity). BFW and source code are publicly available for research and practice.

The BFW data and benchmarks address fairness in the data. Our feature encoder addresses privacy concerns by learning to map faces to a lower dimension that preserves identity and removes subgroup information. BFW is at the forefront of ethical AI [109].

The experimental settings and practice remain an open problem. For instance, gender labels are boolean: an approximation of sexuality that is best represented as real values [70]. Finer-grained, or more precise subgroups, could be another improvement (*e.g.*, Indians from North India versus South India, Black Africans versus African Americans, or distinguishing groups of Africa). Our intent is for BFW to serve as a benchmark of existing systems, and a foundation for future researchers to extend.

## REFERENCES

- [1] A. Acien, A. Morales, R. Vera-Rodriguez, I. Bartolome, and J. Fierrez, “Measuring the gender and ethnicity bias in deep models for face recognition,” in *Progress in Pattern Recognition, Image Analysis, Computer Vision, and Applications*, R. Vera-Rodriguez, J. Fierrez, and A. Morales, Eds. Springer International Publishing, 2019. 1
- [2] L. Anne Hendricks, K. Burns, K. Saenko, T. Darrell, and A. Rohrbach, “Women also snowboard: Overcoming bias in captioning models,” in *Proceedings of the European Conference on Computer Vision*, 2018. 1
- [3] M. Wang, W. Deng, J. Hu, J. Peng, X. Tao, and Y. Huang, “Race faces in-the-wild: Reduce bias by deep unsupervised domain adaptation,” *CoRR arXiv:1812.00194*, 2019. 1, 3, 5
- [4] C. Lazo, “Towards engineering ai software for fairness: A framework to help design fair, accountable and transparent algorithmic decision-making systems,” *TU Delft Library*, 2020. 1
- [5] I. D. Raji and J. Buolamwini, “Actionable auditing: Investigating the impact of publicly naming biased performance results of commercial ai products,” in *Proceedings of the 2019 AAAI/ACM Conference on AI, Ethics, and Society*, 2019, pp. 429–435. 1
- [6] P. Drozdowski, C. Rathgeb, A. Dantcheva, N. Damer, and C. Busch, “Demographic bias in biometrics: A survey on an emerging challenge,” *IEEE Transactions on Technology and Society*, 2020. 1, 2, 3
- [7] J. Deng, J. Guo, N. Xue, and S. Zafeiriou, “Arcface: Additive angular margin loss for deep face recognition,” in *IEEE Conference on Computer Vision and Pattern Recognition (CVPR)*, 2019. 1, 2

- [8] W. Liu, Y. Wen, Z. Yu, M. Li, B. Raj, and L. Song, "Sphereface: Deep hypersphere embedding for face recognition," in *IEEE Conference on Computer Vision and Pattern Recognition (CVPR)*, 2017. 1, 2
- [9] F. Wang, J. Cheng, W. Liu, and H. Liu, "Additive margin softmax for face verification," *IEEE Signal Processing Letters*, 2018. 1, 8
- [10] H. Wang, Y. Wang, Z. Zhou, X. Ji, D. Gong, J. Zhou, Z. Li, and W. Liu, "Cosface: Large margin cosine loss for deep face recognition," in *IEEE Conference on Computer Vision and Pattern Recognition*, 2018. 1
- [11] J. P. Robinson, G. Livitz, Y. Henon, C. Qin, Y. Fu, and S. Timoner, "Face recognition: too bias, or not too bias?" in *Computer Vision and Pattern Recognition Workshop*, 2020, pp. 0–1. 1, 2, 3, 5, 6, 8
- [12] K. W. Bowyer, "Face recognition technology: security versus privacy," *IEEE Technology and society magazine*, pp. 9–19, 2004. 2
- [13] Y. Taigman, M. Yang, M. Ranzato, and L. Wolf, "Deepface: Closing the gap to human-level performance in face verification," in *Conference on Computer Vision and Pattern Recognition*, 2014. 2
- [14] O. M. Parkhi, A. Vedaldi, and A. Zisserman, "Deep face recognition," in *British Machine Vision Conference (BMVC)*, 2015. 2
- [15] Y. Wen, K. Zhang, Z. Li, and Y. Qiao, "A discriminative feature learning approach for deep face recognition," in *European Conference on Computer Vision*, 2016, pp. 499–515. 2
- [16] Y. Duan, J. Lu, and J. Zhou, "Uniformface: Learning deep equidistributed representation for face recognition," in *IEEE Conference on Computer Vision and Pattern Recognition (CVPR)*, 2019. 2
- [17] Z. Wang, G. Wang, B. Huang, Z. Xiong, Q. Hong, H. Wu, P. Yi, K. Jiang, N. Wang, Y. Pei *et al.*, "Masked face recognition dataset and application," *CoRR arXiv:2003.09093*, 2020. 2
- [18] Z. Zhu, G. Huang, J. Deng, Y. Ye, J. Huang, X. Chen, J. Zhu, T. Yang, J. Lu, D. Du, and J. Zhou, "Webface260m: A benchmark unveiling the power of million-scale deep face recognition," in *Proceedings of the IEEE/CVF Conference on Computer Vision and Pattern Recognition (CVPR)*, June 2021, pp. 10492–10502. 2
- [19] G. Guo and N. Zhang, "A survey on deep learning based face recognition," *Computer Vision and Image Understanding*, 2019. 2
- [20] I. Masi, Y. Wu, T. Hassner, and P. Natarajan, "Deep face recognition: A survey," in *2018 31st SIBGRAPI conference on graphics, patterns and images (SIBGRAPI)*. IEEE, 2018, pp. 471–478. 2
- [21] A. Khalil, S. G. Ahmed, A. M. Khattak, and N. Al-Qirim, "Investigating bias in facial analysis systems: A systematic review," *IEEE Access*, vol. 8, pp. 130751–130761, 2020. 2
- [22] J. Buolamwini and T. Gebru, "Gender shades: Intersectional accuracy disparities in commercial gender classification," in *Conference on fairness, accountability and transparency*. PMLR, 2018. 2
- [23] P. Grother, M. Ngan, and K. Hanaoka, "Face recognition vendor test part 3: Demographic effects," 2019-12-19 2019. 2
- [24] V. Muthukumar, T. Pedapati, N. Ratha, P. Sattigeri, C.-W. Wu, B. Kingsbury, A. Kumar, S. Thomas, A. Mojsilovic, and K. R. Varshney, "Understanding unequal gender classification accuracy from face images," *CoRR arXiv:1812.00099*, 2018. 2
- [25] P. Terhörst, J. N. Kolf, M. Huber, F. Kirchbuchner, N. Damer, A. Morales, J. Fierrez, and A. Kuijper, "A comprehensive study on face recognition biases beyond demographics," *CoRR arXiv:2110.08396*, 2021. 2
- [26] G. Balakrishnan, Y. Xiong, W. Xia, and P. Perona, "Towards causal benchmarking of bias in face analysis algorithms," *CoRR arXiv:2007.06570*, 2020. 2
- [27] M. Georgopoulos, J. Oldfield, M. A. Nicolaou, Y. Panagakis, and M. Pantic, "Enhancing facial data diversity with style-based face aging," in *CVPR Workshop*, 2020. 2
- [28] V. Muthukumar, T. Pedapati, N. Ratha, P. Sattigeri, C.-W. Wu, B. Kingsbury, A. Kumar, S. Thomas, A. Mojsilović, and K. R. Varshney, "Color-theoretic experiments to understand unequal gender classification accuracy from face images," in *Computer Vision and Pattern Recognition Workshop*, 2019, pp. 2286–2295. 2
- [29] P. Dhar, J. Gleason, A. Roy, C. D. Castillo, P. J. Phillips, and R. Chellappa, "Distill and de-bias: Mitigating bias in face recognition using knowledge distillation," *CORR arXiv:2112.09786*, 2021. 2
- [30] B. Liu, S. Zhang, G. Song, H. You, and Y. Liu, "Rectifying the data bias in knowledge distillation," in *IEEE International Conference on Computer Vision (ICCV)*, 2021, pp. 1477–1486. 2
- [31] S. Gong, X. Liu, and A. K. Jain, "Mitigating face recognition bias via group adaptive classifier," in *IEEE Conference on Computer Vision and Pattern Recognition (CVPR)*, 2021, pp. 3414–3424. 2
- [32] I. Serna, A. Peña, A. Morales, and J. Fierrez, "Insidebias: Measuring bias in deep networks and application to face gender biometrics," *CoRR arXiv:2004.06592*, 2020. 2
- [33] V. Albiero, K. KS, K. Vangara, K. Zhang, M. C. King, and K. W. Bowyer, "Analysis of gender inequality in face recognition accuracy," in *Computer Vision and Pattern Recognition Workshop*, 2020. 2
- [34] A. Das, A. Dantcheva, and F. Bremond, "Mitigating bias in gender, age and ethnicity classification: a multi-task convolution neural network approach," in *European Conference on Computer Vision*, 2018. 2
- [35] N. Srinivas, K. Ricanek, D. Michalski, D. S. Bolme, and M. King, "Face recognition algorithm bias: Performance differences on images of children and adults," in *Computer Vision and Pattern Recognition Workshop*, 2019. 2
- [36] S. Nagpal, M. Singh, R. Singh, M. Vatsa, and N. Ratha, "Deep learning for face recognition: Pride or prejudiced?" *CoRR arXiv:1904.01219*, 2019. 2
- [37] A. Acien, A. Morales, R. Vera-Rodriguez, I. Bartolome, and J. Fierrez, "Measuring the gender and ethnicity bias in deep models for face recognition," in *Iberoamerican Congress on Pattern Recognition*. Springer, 2018. 2, 10
- [38] S. Gong, X. Liu, and A. K. Jain, "Debiasface: De-biasing face recognition," *CoRR arXiv:1911.08080*, 2019. 2
- [39] A. V. Savchenko, "Efficient facial representations for age, gender and identity recognition in organizing photo albums using multi-output convnet," *PeerJ Computer Science*, vol. 5, p. e197, 2019. 2
- [40] S. Nagpal, M. Singh, R. Singh, and M. Vatsa, "Attribute aware filter-drop for bias invariant classification," in *Computer Vision and Pattern Recognition Workshop*, June 2020. 2
- [41] T. Sixta, J. Junior, C. Jacques, P. Buch-Cardona, E. Vazquez, and S. Escalera, "Fairface challenge at eccv 2020: Analyzing bias in face recognition," *CoRR arXiv:2009.07838*, 2020. 2
- [42] A. Peña, I. Serna, A. Morales, and J. Fierrez, "Bias in multimodal ai: Testbed for fair automatic recruitment," *arXiv:2004.07173*, 2020. 2
- [43] A. Peña, I. Serna, A. Morales, and J. Fierrez, "Faircvtest demo: Understanding bias in multimodal learning with testbed in fair automatic recruitment," *CoRR arXiv:2009.07025*, 2020. 2
- [44] P. Terhörst, N. Damer, F. Kirchbuchner, and A. Kuijper, "Suppressing gender and age in face templates using incremental variable elimination," in *2019 International Conference on Biometrics (ICB)*, 2019, pp. 1–8. 2
- [45] B. Sadeghi and V. N. Boddeti, "Imparting fairness to pre-trained biased representations," in *Computer Vision and Pattern Recognition Workshop*, June 2020. 2
- [46] M. Wang and W. Deng, "Mitigating bias in face recognition using skewness-aware reinforcement learning," in *IEEE Conference on Computer Vision and Pattern Recognition (CVPR)*, 2020. 2
- [47] P.-M. Law, S. Malik, F. Du, and M. Sinha, "Designing tools for semi-automated detection of machine learning biases: An interview study," *CoRR arXiv:2003.07680*, 2020. 2
- [48] P. Terhörst, J. N. Kolf, N. Damer, F. Kirchbuchner, and A. Kuijper, "Post-comparison mitigation of demographic bias in face recognition using fair score normalization," *CoRR arXiv:2002.03592*, 2020. 3
- [49] J. G. Cavazos, P. J. Phillips, C. D. Castillo, and A. J. O'Toole, "Accuracy comparison across face recognition algorithms: Where are we on measuring race bias?" *IEEE transactions on biometrics, behavior, and identity science*, vol. 3, no. 1, pp. 101–111, 2020. 3
- [50] Z. Khan and Y. Fu, "One label, one billion faces: Usage and consistency of racial categories in computer vision," in *Proceedings of the 2021 ACM Conference on Fairness, Accountability, and Transparency*. Association for Computing Machinery, 2021. 3, 6
- [51] C. Drummond, R. C. Holte *et al.*, "C4. 5, class imbalance, and cost sensitivity: why under-sampling beats over-sampling," in *Workshop on learning from imbalanced datasets II*. Citeseer, 2003. 3
- [52] S. Gong, X. Liu, and A. K. Jain, "Mitigating face recognition bias via group adaptive classifier," in *IEEE Conference on Computer Vision and Pattern Recognition (CVPR)*, June 2021, pp. 3414–3424. 3
- [53] Z. Yang, X. Zhu, C. Jiang, W. Liu, and L. Shen, "Ramface: Race adaptive margin based face recognition for racial bias mitigation," in *International Joint Conference on Biometrics (IJCB)*. IEEE, 2021. 3
- [54] M. Oquab, L. Bottou, I. Laptev, and J. Sivic, "Learning and transferring mid-level image representations using convolutional neural networks," in *IEEE Conference on Computer Vision and Pattern Recognition (CVPR)*, 2014, pp. 1717–1724. 3
- [55] E. M. Rudd, M. Günther, and T. E. Boulton, "Moon: A mixed objective optimization network for the recognition of facial attributes," in *European Conference on Computer Vision*. Springer, 2016. 3
- [56] C. Huang, Y. Li, C. L. Chen, and X. Tang, "Deep imbalanced learning for face recognition and attribute prediction," *IEEE Transactions on Pattern Analysis and Machine Intelligence (TPAMI)*, 2019. 3

- [57] T. Wang, J. Zhao, M. Yatskar, K.-W. Chang, and V. Ordonez, "Balanced datasets are not enough: Estimating and mitigating gender bias in deep image representations," in *IEEE International Conference on Computer Vision (ICCV)*, 2019, pp. 5310–5319. 3
- [58] H. He and E. A. Garcia, "Learning from imbalanced data," *IEEE Transactions on knowledge and data engineering*, 2009. 3
- [59] H. He and Y. Ma, *Imbalanced learning: foundations, algorithms, and applications*. John Wiley & Sons, 2013. 3
- [60] B. Krawczyk, "Learning from imbalanced data: open challenges and future directions," *Progress in Artificial Intelligence*, 2016. 3
- [61] T. Xu, J. White, S. Kalkan, and H. Gunes, "Investigating bias and fairness in facial expression recognition," *arXiv:2007.10075*, 2020. 3
- [62] M. Gwilliam, S. Hegde, L. Tinubu, and A. Hanson, "Rethinking common assumptions to mitigate racial bias in face recognition datasets," in *International Conference on Computer Vision (ICCV) Workshop*, October 2021, pp. 4123–4132. 3
- [63] V. Albiero, K. Zhang, and K. Bowyer, "How gender balance in training data affect face recognition accuracy?" *arXiv:2002.02934*, 2020. 3
- [64] Y. Guo, L. Zhang, Y. Hu, X. He, and J. Gao, "Ms-celeb-1m: A dataset and benchmark for large-scale face recognition," in *European Conference on Computer Vision*, 2016. 3, 8
- [65] F. Schroff, D. Kalenichenko, and J. Philbin, "Facenet: A unified embedding for face recognition and clustering," in *IEEE Conference on Computer Vision and Pattern Recognition (CVPR)*, 2015. 3
- [66] Q. Cao, L. Shen, W. Xie, O. M. Parkhi, and A. Zisserman, "Vggface2: A dataset for recognising faces across pose and age," in *IEEE International Conference on Automatic Face and Gesture Recognition*, 2018. 3, 5
- [67] B. Maze, J. Adams, J. A. Duncan, N. Kalka, T. Miller, C. Otto, A. K. Jain, W. T. Niggel, J. Anderson, J. Cheney *et al.*, "Iarpa janus benchmark-c: Face dataset and protocol," in *2018 International Conference on Biometrics (ICB)*. IEEE, 2018, pp. 158–165. 3
- [68] I. Hupont and C. Fernández, "Demogpairs: Quantifying the impact of demographic imbalance in deep face recognition," in *Conference on Automatic Face and Gesture Recognition*. IEEE, 2019. 3, 5
- [69] K. Kärkkäinen and J. Joo, "Fairface: Face attribute dataset for balanced race, gender, and age," *Winter Conference on Applications of Computer Vision (WACV)*, 2021. 3, 5
- [70] M. Merler, N. Ratha, R. S. Feris, and J. R. Smith, "Diversity in faces," *CoRR arXiv:1901.10436*, 2019. 3, 11
- [71] D. Yi, Z. Lei, S. Liao, and S. Z. Li, "Learning face representation from scratch," *CoRR arXiv:1411.7923*, 2014. 3
- [72] Z. Ding, S. Li, M. Shao, and Y. Fu, "Graph adaptive knowledge transfer for unsupervised domain adaptation," in *ECCV*, 2018. 3
- [73] X. Peng, B. Usman, N. Kaushik, J. Hoffman, D. Wang, and K. Saenko, "Visda: The visual domain adaptation challenge," *CoRR arXiv:1710.06924*, 2017. 3
- [74] K. Saito, D. Kim, S. Sclaroff, T. Darrell, and K. Saenko, "Semi-supervised domain adaptation via minimax entropy," *CoRR arXiv:1904.06487*, 2019. 3, 4
- [75] R. Shu, H. H. Bui, H. Narui, and S. Ermon, "A dirt-t approach to unsupervised domain adaptation," *arXiv:1802.08735*, 2018. 4
- [76] B. Sun and K. Saenko, "Subspace distribution alignment for unsupervised domain adaptation," in *BMVC*, 2015. 4
- [77] M. Long, J. Wang, G. Ding, J. Sun, and P. S. Yu, "Transfer feature learning with joint distribution adaptation," in *ICCV*, 2013. 4
- [78] B. Gong, Y. Shi, F. Sha, and K. Grauman, "Geodesic flow kernel for unsupervised domain adaptation," in *CVPR*, 2012. 4
- [79] R. Gopalan, R. Li, and R. Chellappa, "Domain adaptation for object recognition: An unsupervised approach," in *ICCV*, 2011. 4
- [80] Y. Ganin, E. Ustinova, H. Ajakan, P. Germain, H. Larochelle, F. Laviolette, M. Marchand, and V. Lempitsky, "Domain-adversarial training of neural networks," *JMLR*, vol. 17, no. 1, 2016. 4
- [81] E. Tzeng, J. Hoffman, K. Saenko, and T. Darrell, "Adversarial discriminative domain adaptation," in *CVPR*, 2017. 4
- [82] B. H. Zhang, B. Lemoine, and M. Mitchell, "Mitigating unwanted biases with adversarial learning," in *Proceedings of the AAAI/ACM Conference on AI, Ethics, and Society*, 2018, pp. 335–340. 4
- [83] P. Dhar, J. Gleason, H. Sourì, C. D. Castillo, and R. Chellappa, "An adversarial learning algorithm for mitigating gender bias in face recognition," *CoRR arXiv:2006.07845*, 2020. 4
- [84] V. Mirjalili, S. Raschka, and A. Ross, "Gender privacy: An ensemble of semi adversarial networks for confounding arbitrary gender classifiers," in *2018 IEEE 9th International Conference on Biometrics Theory, Applications and Systems (BTAS)*, 2018, pp. 1–10. 4
- [85] J. Hamm, "Minimax filter: Learning to preserve privacy from inference attacks," *The Journal of Machine Learning Research*, 2017. 4
- [86] M. Bertran, N. Martinez, A. Papadaki, Q. Qiu, M. Rodrigues, G. Reeves, and G. Sapiro, "Adversarially learned representations for information obfuscation and inference," in *International Conference on Machine Learning (ICML)*. PMLR, 2019, pp. 614–623. 4
- [87] P. C. Roy and V. N. Boddeti, "Mitigating information leakage in image representations: A maximum entropy approach," in *IEEE Conference on Computer Vision and Pattern Recognition (CVPR)*, 2019. 4
- [88] Z. Wu, H. Wang, Z. Wang, H. Jin, and Z. Wang, "Privacy-preserving deep action recognition: An adversarial learning framework and a new dataset," *IEEE Transactions on Pattern Analysis and Machine Intelligence (TPAMI)*, pp. 1–1, 2020. 4
- [89] Z. Wu, Z. Wang, Z. Wang, and H. Jin, "Towards privacy-preserving visual recognition via adversarial training: A pilot study," in *European Conference on Computer Vision*, 2018, pp. 606–624. 4
- [90] A. Othman and A. Ross, "Privacy of facial soft biometrics: Suppressing gender but retaining identity," in *Computer Vision - ECCV 2014 Workshops*, L. Agapito, M. M. Bronstein, and C. Rother, Eds. Cham: Springer International Publishing, 2015, pp. 682–696. 4
- [91] S. Guo, T. Xiang, and X. Li, "Towards efficient privacy-preserving face recognition in the cloud," *Signal Processing*, pp. 320 – 328, 2019. 4
- [92] Z. Ma, Y. Liu, X. Liu, J. Ma, and K. Ren, "Lightweight privacy-preserving ensemble classification for face recognition," *IEEE Internet of Things Journal*, vol. 6, no. 3, pp. 5778–5790, 2019. 4
- [93] P. Dhar, J. Gleason, A. Roy, C. D. Castillo, and R. Chellappa, "Pass: Protected attribute suppression system for mitigating bias in face recognition," in *IEEE International Conference on Computer Vision (ICCV)*, 2021, pp. 15 087–15 096. 4
- [94] A. Ambekar, C. Ward, J. Mohammed, S. Male, and S. Skiena, "Name-ethnicity classification from open sources," in *Proceedings of SIGKDD conference on Knowledge Discovery and Data Mining*, 2009. 5
- [95] S. Fu, H. He, and Z.-G. Hou, "Learning race from face: A survey," *Transactions on Pattern Analysis and Machine Intelligence*, 2014. 5
- [96] G. Levi and T. Hassner, "Age and gender classification using convolutional neural networks," in *Computer Vision and Pattern Recognition Workshop*, 2015, pp. 34–42. 5
- [97] Y. Ganin and V. Lempitsky, "Unsupervised domain adaptation by backpropagation," in *International Conference on Machine Learning (ICML)*. PMLR, 2015, pp. 1180–1189. 6, 7
- [98] M. Yudell, D. Roberts, R. DeSalle, and S. Tishkoff, "Taking race out of human genetics," *Science*, 2016. 5
- [99] M. O. Hill, "Diversity and evenness: a unifying notation and its consequences," *Ecology*, vol. 54, no. 2, pp. 427–432, 1973. 6
- [100] S. Eilers, D. Q. Bach, R. Gaber, H. Blatt, Y. Guevara, K. Nitsche, R. V. Kundu, and J. K. Robinson, "Accuracy of Self-report in Assessing Fitzpatrick Skin Phototypes I Through VI," *JAMA Dermatology*, vol. 149, no. 11, pp. 1289–1294, 11 2013. 6
- [101] N. M. Kinyanjui, T. Odonga, C. Cintas, N. C. F. Codella, R. Panda, P. Sattigeri, and K. R. Varshney, "Estimating skin tone and effects on classification performance in dermatology datasets," *CoRR*, vol. abs/1910.13268, 2019. 6
- [102] H. V. Nguyen and L. Bai, "Cosine similarity metric learning for face verification," in *Asian Conference on Computer Vision (ACCV)*. Springer, 2010, pp. 709–720. 6
- [103] G. B. Huang, M. Ramesh, T. Berg, and E. Learned-Miller, "Labeled faces in the wild: A database for studying face recognition in unconstrained environments," *UMass, Tech. Rep.*, 2007. 7, 8
- [104] K. Zhang, Z. Zhang, Z. Li, and Y. Qiao, "Joint face detection and alignment using multitask cascaded convolutional networks," *Signal Processing Letters*, 2016. 8
- [105] F. Wang, X. Xiang, J. Cheng, and A. L. Yuille, "Normface: L2 hypersphere embedding for face verification," in *ACM Conference on Multimedia*, 2017, pp. 1041–1049. 8
- [106] N. Srivastava, G. Hinton, A. Krizhevsky, I. Sutskever, and R. Salakhutdinov, "Dropout: a simple way to prevent neural networks from overfitting," *The journal of machine learning research*, vol. 15, no. 1, pp. 1929–1958, 2014. 10
- [107] D. P. Kingma and J. Ba, "Adam: A method for stochastic optimization," *CoRR arXiv:1412.6980*, 2014. 10
- [108] L. A. Jeni, J. F. Cohn, and F. De La Torre, "Facing imbalanced data—recommendations for the use of performance metrics," in *Humaine association conference on affective computing and intelligent interaction*. IEEE, 2013, pp. 245–251. 10
- [109] M. Hanley, A. Khandelwal, H. Averbuch-Elor, N. Snaveley, and H. Nissenbaum, "An ethical highlighter for people-centric dataset creation," in *Advances in Neural Information Processing Systems (NIPS) Workshop*, 2020. 11